

Robust Gaussian Filtering

Manuel Wüthrich¹, Cristina Garcia Cifuentes¹, Sebastian Trimpe¹
 Franziska Meier², Jeannette Bohg¹, Jan Issac¹ and Stefan Schaal^{1,2}

Abstract—Most widely-used state estimation algorithms, such as the Extended Kalman Filter and the Unscented Kalman Filter, belong to the family of Gaussian Filters (GF). Unfortunately, GFs fail if the measurement process is modelled by a fat-tailed distribution. This is a severe limitation, because thin-tailed measurement models, such as the analytically-convenient and therefore widely-used Gaussian distribution, are sensitive to outliers. In this paper, we show that mapping the measurements into a specific feature space enables any existing GF algorithm to work with fat-tailed measurement models. We find a feature function which is optimal under certain conditions. Simulation results show that the proposed method allows for robust filtering in both linear and nonlinear systems with measurements contaminated by fat-tailed noise.

I. INTRODUCTION

Robust and accurate state estimation is essential to safely control any dynamical system. Most widely used estimation algorithms, such as the Extended Kalman Filter (EKF) [24] and the Sigma Point Kalman Filters (SPKF) [27], belong to the family of Gaussian Filters (GF). However, GFs are inherently non-robust against outliers, since the mean estimate scales linearly with the measurement. This is problematic because many sensors, such as range, sonar, radar, GPS and visual devices, provide measurements populated with outliers.

In this paper we argue that problems with outliers are a direct consequence of unrealistic, thin-tailed measurement models. Unfortunately, GFs are inherently unable to perform accurate estimation with more realistic, fat-tailed measurement models. Therefore, we propose a method which enables any member of the family of GFs to work with fat-tailed measurement models by applying one simple change: Instead of filtering with the physical measurement, we filter with a virtual measurement. This virtual measurement is obtained by applying a time-varying feature function to the physical measurement. We derive a feature function which is optimal under some conditions. In simulation experiments, we demonstrate the robustness and accuracy of the proposed method for linear as well as nonlinear systems. We compare the performance of the proposed method and the standard GF.

II. RELATED WORK

Ad-hoc procedures for reducing the influence of outliers have been employed by engineers for a long time. One such heuristic is to simply discard all measurements which are

too far away from the expected measurement. This approach lacks a firm theoretical basis and there is no rigorous way of choosing the thresholds. Furthermore, the information contained in measurements outside of the thresholds is discarded completely, which can lead to decreased efficiency [23].

For these reasons, significant research effort has been devoted to robustifying GFs in a principled manner. There are two main currents in the literature on robust filtering. The first tries to directly find estimators which are robust to small deviations from Gaussian noise. The second approach is to find the posterior estimate given a fat-tailed measurement model.

A. Robust Estimators

The literature on robust statistics is vast and due to space constraints we cannot provide an exhaustive review. Instead, we discuss a few relevant and representative examples for approaches that are based on robust estimators in the spirit of [9]. In this framework, the objective is to find an estimator with a small variance when the Gaussian noise is contaminated with noise from a broad class of distributions. Masreliez and Martin [16] propose such an estimator for linear systems. This approach is extended by Schick and Mitter [23].

B. Fat-tailed Measurement Models

Since fat-tailed measurement models are by definition non-Gaussian, finding the posterior estimate is not trivial. In particular, a lot of effort has been devoted to finding filtering recursions for models with Student t -distributed noise.

Roth et al. [20] show that for linear systems where the noise and the state are jointly t -distributed, an exact filter can be found. The authors mention that these noise conditions are rarely met in filtering problems, and propose an approximation for state-independent t -distributed noise. A different approximation scheme for linear systems with t -distributed noise is proposed in Meinhold and Singpurwalla [17].

While those approximations are hand-crafted, Ting et al. [26] and Särkkä and Nummenmaa [22] use variational inference techniques to find an optimal approximation to the posterior. Agamennoni et al. [1] unify and generalize those methods.

C. Extensions to Nonlinear Systems

All methods mentioned above assume a linear measurement model. It is possible to apply them to nonlinear systems by linearising the measurement model at each time step, as is done in the EKF. However, SPKFs have been shown

¹ Autonomous Motion Department at the Max Planck Institute for Intelligent Systems, Tübingen, Germany. Email: first.lastname@tuebingen.mpg.de

² Computational Learning and Motor Control lab at the University of Southern California, Los Angeles, CA, USA.

to yield superior performance for many nonlinear systems [27, 11, 10].

Applying the robustification methods discussed so far to SPKFs is not as simple. One way of doing so is proposed by Karlgaard and Schaub [14], who use a robust Huber estimator [9] in a SPKF. Similarly, Piche et al. [19] propose a method of applying the fat-tailed filtering methods mentioned to SPKFs.

However, both of these methods rely on an iterative optimization at each time step, which is computationally expensive. In contrast, the robustification proposed in this paper allows the application of any of the numerous GF algorithms, be it EKF or SPKF. The only required change is to transform the measurement into a feature space before applying the filter.

III. FILTERING

A discrete-time state-space model can be defined by two probability distributions: a state transition model $p(x_t|x_{t-1})$, which describes the evolution of the state in time, and a measurement model $p(y_t|x_t)$, which describes how the measurement y_t is generated given the state x_t . Alternatively, these two models can also be written in functional form

$$x_t = g(x_{t-1}, v_t) \quad (1)$$

$$y_t = h(x_t, w_t) \quad (2)$$

with v_t and w_t being standard normal noise. Note that any (even non-Gaussian) model can be specified in this way, since the Gaussian noise can be mapped onto any desired distribution inside the nonlinear functions $g(\cdot)$ and $h(\cdot)$.

A. Exact Filtering

Filtering is concerned with estimating the current state x_t given all past measurements $y_{1:t}$. The posterior distribution of the current state $p(x_t|y_{1:t})$ can be computed recursively from the distribution of the previous state $p(x_{t-1}|y_{1:t-1})$. This recursion can be written in two steps, a prediction step¹

$$p(x_t|y_{1:t-1}) = \int_{x_{t-1}} p(x_t|x_{t-1})p(x_{t-1}|y_{1:t-1}) \quad (3)$$

and an update step

$$p(x_t|y_{1:t}) = \frac{p(y_t|x_t)p(x_t|y_{1:t-1})}{\int_{x_t} p(y_t|x_t)p(x_t|y_{1:t-1})}. \quad (4)$$

The equations above can generally not be solved in closed form [15]. The most notable exception is the Kalman Filter (KF) [13], which provides the exact solution for linear Gaussian systems. Significant research effort has been invested into generalizing the KF to nonlinear dynamical systems. The KF and its generalizations to nonlinear systems can be seen as members of the family of GFs [29, 10, 21, 30].

B. Gaussian Filtering

GFs approximate both the predicted belief (3), as well as the posterior belief (4) with Gaussian distributions.

In the prediction step (3), the exact distribution is approximated by a Gaussian²

$$p(x_t|y_{1:t-1}) = \mathcal{N}(x_t|\mu_{x_t}, \Sigma_{x_t x_t}). \quad (5)$$

The prediction step is not affected by the type of measurement model used, and will therefore not be discussed here, see for instance [21, 30, 10, 29] for more details.

We will only consider the update step (4) in the remainder of the paper. For ease of notation we will not write the dependence on past measurements $y_{1:t-1}$ explicitly any more. The remaining variables all have time index t , which can therefore be dropped. The predicted belief $p(x_t|y_{1:t-1})$ can now simply be written as $p(x)$, and the posterior belief $p(x_t|y_{1:t})$ as $p(x|y)$ etc.

As shown in [30], the GF can be understood as finding an approximate Gaussian posterior $q(x|y)$ by minimizing the Kullback-Leibler divergence

$$\text{KL}[p(x, y)|q(x|y)] \quad (6)$$

to the exact joint distribution. The form of $q(x|y)$ is restricted to be Gaussian in x

$$q(x|y) = \mathcal{N}(x|m(y), \Sigma) \quad (7)$$

with the mean being an affine function of y

$$m(y) = M \begin{pmatrix} 1 \\ y \end{pmatrix}. \quad (8)$$

This minimization is performed at each update step and yields the optimal parameters of the approximation (7)

$$M = (\mu_x - \Sigma_{xy}\Sigma_{yy}^{-1}\mu_y \quad \Sigma_{xy}\Sigma_{yy}^{-1}) \quad (9)$$

$$\Sigma = \Sigma_{xx} - \Sigma_{xy}\Sigma_{yy}^{-1}\Sigma_{xy}^T. \quad (10)$$

See [30] for a detailed derivation of this result. The parameters μ_x and Σ_{xx} are given by (5). The remaining parameters are defined as

$$\mu_y = \int_y y p(y) \quad (11)$$

$$\Sigma_{yy} = \int_y (y - \mu_y)(y - \mu_y)^T p(y) \quad (12)$$

$$\Sigma_{xy} = \int_{x,y} (x - \mu_x)(y - \mu_y)^T p(x, y). \quad (13)$$

For a linear system, this solution corresponds to the Kalman filter equations [30].

1) *Numeric Integration Methods:* For most nonlinear systems, these integrals have to be approximated. In the EKF, this is done by linearisation at the current estimate of the state x . This approximation does not take the uncertainty in the estimate into account, which can lead to large errors and sometimes even divergence of the filter [27, 10].

Therefore, approximations based on numeric integration methods are preferable in most cases. Deterministic Gaussian integration schemes have been investigated thoroughly, and the resulting filters are collected under the term Sigma Point Kalman Filters (SPKF) [27]. Well known members of

¹We use the notation $\int_x(\cdot)$ as an abbreviation for $\int_{-\infty}^{\infty}(\cdot)dx$.

² $\mathcal{N}(z|\mu, \Sigma)$ denotes the Gaussian with mean μ and covariance Σ .

this family are the Unscented Kalman Filter (UKF) [11], the Divided Difference Filter (DDF) [18] and the Cubature Kalman Filter (CKF) [2]. Alternatively, numeric integration can also be performed using Monte Carlo methods. The ideas presented in this paper apply to any GF, regardless of which particular integration method is used.

IV. A CASE FOR FAT TAILS

Measurement acquisition is typically modelled by a Gaussian or some other thin-tailed measurement model. This assumption is usually made for analytical convenience, not because it is an accurate representation of the belief of the engineer. If an engineer were to believe that measurements are in fact generated by a Gaussian distribution, then she would have to accept a betting ratio of 7×10^{14} to 1 that no measurement further than 8 standard deviations from the state will occur³. Few engineers would be interested in such a bet, since one can usually not exclude the possibility of acquiring a large measurement due to unexpected physical effects.

The mismatch between the actual belief and the Gaussian model can lead to counter-intuitive behaviour of the inference algorithm. More concretely, the posterior mean is an affine function of the measurement. This means the shift in the mean produced by a single measurement is not bounded.

This problem is easily addressed by using a more realistic, fat-tailed model [17]. There are several definitions of fat-tails which are commonly used [5]. Here, we simply mean any distribution which decays slower than the Gaussian. Which particular tail model is used depends on the application.

A. The Gaussian Filter using Fat Tails

The GF approximates all beliefs with Gaussians, but the measurement model can have any form. In principle, nothing prevents us from using the GF with a fat-tailed measurement model. Unfortunately, the GF is not able to do proper inference using such a model. The measurement model enters the GF equations only through (11), (12) and (13). To see which properties of the measurement model are relevant for the GF, we rewrite these equations and integrate in y

$$\mu_y = \int_x \mu_{y|x}(x) p(x) \quad (14)$$

$$\Sigma_{yy} = \int_x (\Sigma_{yy|x}(x) + \mu_{y|x}(x) \mu_{y|x}(x)^\top - \mu_y \mu_y^\top) p(x) \quad (15)$$

$$\Sigma_{xy} = \int_x (x - \mu_x) (\mu_{y|x}(x) - \mu_y)^\top p(x). \quad (16)$$

What is important to note here is that these equations only depend on the measurement model through the conditional mean and the conditional covariance

$$\mu_{y|x}(x) = \int_y y p(y|x) \quad (17)$$

$$\Sigma_{yy|x}(x) = \int_y (y - \mu_{y|x}(x)) (y - \mu_{y|x}(x))^\top p(y|x). \quad (18)$$

Since fat-tailed measurement models typically have very large or even infinite covariances, the GF will behave as if the

³According to De Finetti's definition of probability [6].

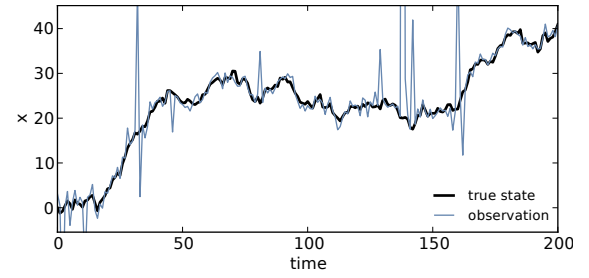


Fig. 1: Simulation of the system described in Example 4.1.

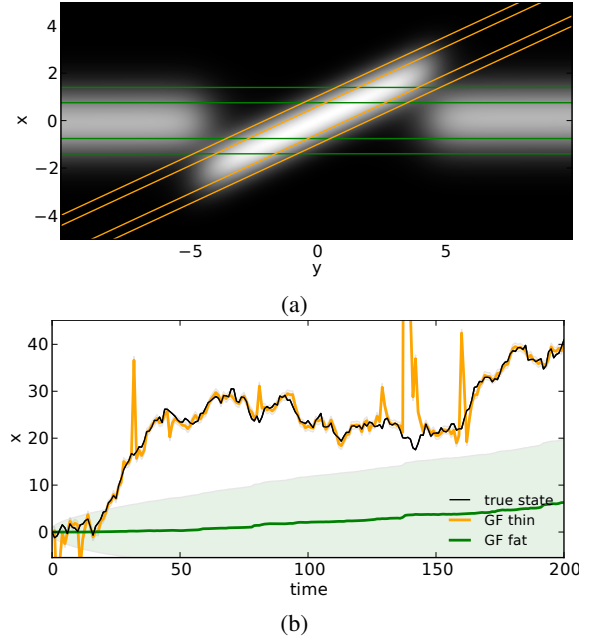


Fig. 2: Standard GF applied to a fat-tailed measurement process. (a) The exact density $p(x_1|y_1)$ (white) overlaid with contour lines of the approximate density $q(x_1|y_1)$ given by a fat-tailed GF (green) and a thin-tailed GF (orange). (b) True state of the system over time, with the obtained estimates.

measurements were extremely noisy. It achieves robustness by simply discarding all measurements, which is not exactly the behaviour we were hoping for.

B. Simulation Example

To illustrate this problematic behaviour, we apply the GF to the following dynamical system:

Example 4.1: System specification⁴

$$p(x_t|x_{t-1}) = \mathcal{N}(x_t|x_{t-1}, 1) \quad (19)$$

$$p(y_t|x_t) = 0.9 \mathcal{N}(y_t|x_t, 1) + 0.1 \mathcal{C}(y_t|x_t, 10) \quad (20)$$

$$p(x_0) = \mathcal{N}(x_0|0, 1) \quad (21)$$

The measurements are contaminated with Cauchy-distributed noise, which leads to occasional outliers, as shown in Figure 1.

We apply two GFs to this problem. The first uses a measurement model which does not take into account the

⁴ $\mathcal{C}(z|\mu, \gamma)$ denotes the Cauchy distribution with location μ and scale γ .

fat-tailed Cauchy noise, it only models the Gaussian noise. The second GF uses a measurement model which is identical to the true measurement process. We will refer to the first filter as the thin-tailed GF, and to the second filter as the fat-tailed GF.

In Figure 2a, we show the exact density $p(x_1|y_1)$ after the first filtering step. The approximations obtained by the thin-tailed GF (yellow) and the fat-tailed GF (green) are overlaid. It can be seen that the approximation to the exact posterior is very poor in both cases.

In the exact density, the function from y to x is approximately linear for small y , and then flattens out for large y . This behaviour cannot be captured by an approximation of the form of (8), since it only allows for linear dependences in y . Hence the poor fit, which leads to an approximation which is essentially independent of y in the case of the fat-tailed GF, and which is very sensitive to extreme values of y in the case of the thin-tailed GF. In both cases, this translates to poor filtering performance, as shown in Figure 2b.

V. A MEASUREMENT FEATURE FOR ROBUSTIFICATION

To enable the GF to work with fat-tailed measurement models, we hence have to change the form of the approximate belief (7). In [30] it is shown that more flexible approximations can be obtained by allowing for nonlinear features in y . The mean function (8) then becomes

$$m(y) = M \left(\frac{1}{\varphi(y)} \right). \quad (22)$$

The resulting filter is equivalent to the standard GF using a virtual measurement which is obtained by applying a nonlinear feature function $\varphi(\cdot)$ to the physical measurement y . Note that this feature function can be time-varying, and may depend on the current belief.

In the following, we address the question of which feature $\varphi(\cdot)$ should be chosen to enable the GF to work with fat-tailed measurement models. Instead of hand-designing such a feature, we attempt to find a feature which is optimal in the sense of (6).

For this purpose, we first find the optimal, non-parametric mean function $m^*(y)$ with respect to (6). Knowing that the mean $m(y)$ is an affine function (22) of the feature $\varphi(y)$, we can then deduce the optimal feature function $\varphi^*(y)$.

A. The Optimal Mean Function

The goal is to find the free form mean function $m^*(y)$ which minimizes (6). To do so, we rewrite the objective (6)

$$\text{KL}[p(x, y)|q(x|y)] = \int_{x, y} \log \left(\frac{p(x, y)}{q(x|y)} \right) p(x, y) \quad (23)$$

$$= \int_y \text{KL}[p(x|y)|q(x|y)] p(y) + C \quad (24)$$

where we have collected the terms which do not depend on the approximation $q(x|y)$ in C . Since there is no constraint on $m^*(y)$, it can be optimized for each y independently. This means that the integral in (24) can be dropped, and we can simply minimize the integrand $\text{KL}[p(x|y)|q(x|y)]$

with respect to $m(y)$. It is a standard result from variational inference that the optimal parameters of a Gaussian approximation are obtained by moment matching [3]. That is, the optimal mean function $m^*(y)$ of the approximation is simply equal to the exact posterior mean

$$m^*(y) = \mu_{x|y}(y) = \int_x xp(x|y). \quad (25)$$

Therefore, ideally, the feature vector $\varphi(y)$ would be such that $\mu_{x|y}(y)$ could be expressed through a linear combination of features. Unfortunately, $\mu_{x|y}(y)$ cannot be found in closed form in most cases.

The standard GF represents the mean of the posterior as an affine function of y . This form is optimal for linear Gaussian systems, and it serves as a good approximation for many nonlinear thin-tailed systems. Similarly, the idea here is to find the optimal feature for a linear Gaussian system with an additive fat tail. This feature can be expected to provide a good approximation for nonlinear fat-tailed systems.

B. The Optimal Feature for a Linear Model with Fat Tails

Suppose that we have a linear Gaussian measurement model

$$b(y|x) = \mathcal{N}(y|Ax + a, P) \quad (26)$$

to which we refer to as the body. We would like to add a fat tail $t(\cdot)$ to make it robust to outliers. The combined measurement model with tail weight $0 \leq \omega \leq 1$ is then

$$p(y|x) = (1 - \omega)b(y|x) + \omega t(y|x). \quad (27)$$

1) *Assumptions On the Form of the Tail:* The shape of the tail depends on the application. For example, Thrun et al. [25] suggest to use a uniform tail on the interval of possible measurements for range sensors. For some other sensors, such an interval is not as well defined, and a tail which assigns a non-zero probability everywhere might be more appropriate.

The precise shape of the tail does not matter for the following derivation. However, we assume it to be almost constant in x on the length scale of the standard deviation of the belief $p(x)$. This is a reasonable assumption, since all the strong dependences of y on x are captured by the body $b(\cdot)$ of the distribution.

This allows us to treat $p(x)$ like a Dirac function with respect to $t(y|x)$ in the subsequent derivation. More concretely, we will use the approximation

$$\int_x f(x)t(y|x)p(x) \approx t(y|\mu_x) \int_x f(x)p(x), \quad (28)$$

where $f(x)$ is an arbitrary function.

For the uniform tails mentioned above, (28) is exact. For state-dependent tails, we expect this approximation to be accurate enough to provide insights into the required form of the feature.

2) *The Conditional Mean:* We will now find the posterior mean $\mu_{x|y}(y)$ for this measurement model, which will then allow us to find the optimal feature. The posterior mean can be obtained from the predicted belief $p(x)$ and the

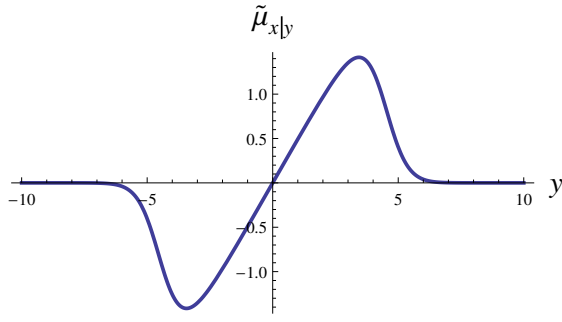


Fig. 3: The approximate optimal mean function (32) for the first measurement of the dynamical system from Example 4.1.

measurement model $p(y|x)$ using Bayes' rule

$$\mu_{x|y}(y) = \int_x xp(x|y) = \frac{\int_x xp(y|x)p(x)}{\int_x p(y|x)p(x)}. \quad (29)$$

Inserting (27) we obtain

$$\mu_{x|y}(y) = \frac{(1-\omega) \int_x xb(y|x)p(x) + \omega \int_x xt(y|x)p(x)}{(1-\omega) \int_x b(y|x)p(x) + \omega \int_x t(y|x)p(x)}. \quad (30)$$

Both the predicted belief $p(x) = \mathcal{N}(x|\mu_x, \Sigma_{xx})$ and the body of the measurement model $b(y|x)$ are Gaussian. Therefore, the integrals on the left hand side of the numerator as well as the denominator can be solved analytically. The integrals on the right side can be approximated according to (28), which yields

$$\mu_{x|y}(y) \approx \tilde{\mu}_{x|y}(y) \quad (31)$$

$$= \frac{(1-\omega)(d + Dy)\mathcal{N}(y|\mu_y^b, \Sigma_{yy}^b) + \omega\mu_x t(y|\mu_x)}{(1-\omega)\mathcal{N}(y|\mu_y^b, \Sigma_{yy}^b) + \omega t(y|\mu_x)} \quad (32)$$

where we have defined

$$D = (\Sigma_{xx}^{-1} + A^\top P^{-1}A)^{-1}A^\top P^{-1} \quad (33)$$

$$d = (\Sigma_{xx}^{-1} + A^\top P^{-1}A)^{-1}(\Sigma_{xx}^{-1}\mu_x - A^\top P^{-1}a). \quad (34)$$

This result has been obtained using standard Gaussian marginalization and conditioning, we therefore skipped the intermediate steps. The expectations

$$\begin{aligned} \mu_y^b &= \int_x \int_y yb(y|x)p(x) \\ \Sigma_{yy}^b &= \int_x \int_y (y - \mu_y^b)(y - \mu_y^b)^\top b(y|x)p(x) \end{aligned} \quad (35)$$

are computed with respect the body only, and are therefore not huge or even infinite, as may be the case for the full measurement model.

In Figure 3 we plot the optimal mean function (32) for the first measurement of the dynamical system from Example 4.1. For measurements y close to the expected measurement $\mu_y = 0$, the conditional mean (32) is approximately linear in y . If a large measurement y is obtained, then the tail becomes predominant, and the posterior mean reverts to the

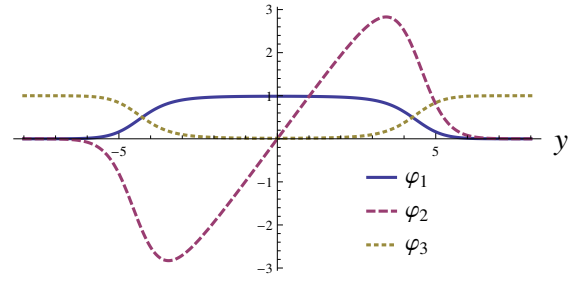


Fig. 4: The optimal feature (36) for the first measurement of the dynamical system from Example 4.1.

prior mean $\mu_x = 0$.

The standard GF attempts to approximate this function by an affine function (8). Not surprisingly, this yields very poor results, as shown in Figure 2a.

3) *The Optimal Feature:* Writing the optimal mean (32) in the form of (22)

$$m^*(y) = \mu_{x|y}(y) \approx \tilde{\mu}_{x|y}(y) = \overbrace{\begin{pmatrix} 0 & d & D & \mu_x \end{pmatrix}}^M \begin{pmatrix} 1 \\ \varphi(y) \end{pmatrix}$$

we can identify the feature

$$\varphi(y) = \frac{\begin{pmatrix} (1-\omega)\mathcal{N}(y|\mu_y^b, \Sigma_{yy}^b) \\ y(1-\omega)\mathcal{N}(y|\mu_y^b, \Sigma_{yy}^b) \\ \omega t(y|\mu_x) \end{pmatrix}}{(1-\omega)\mathcal{N}(y|\mu_y^b, \Sigma_{yy}^b) + \omega t(y|\mu_x)}. \quad (36)$$

In Figure 4 we plot the three dimension of this feature for the Example 4.1. All of the feature components are asymptotically constant in y , which means that the estimate will not grow indefinitely with the measurements. The three components have intuitive interpretations. The first two components are approximately constant $\varphi_1(y)$ and linear $\varphi_2(y)$ in y , for measurements close to the expected value. Hence, they allow the filter to express an affine dependence on y which will vanish for very large measurements. The third component, $\varphi_3(y)$, is small for y close to the expected value, and grows up to some constant for y which are far away. It hence allows the mean estimate to revert to a certain value for large measurements.

For the special case of $\omega = 0$, the feature becomes

$$\varphi(y) = (1, y, 0)^\top. \quad (37)$$

If the measurement model does not have a fat tail, the standard Gaussian Filter is thus retrieved. The linear mean function (8) is a special case of the featurised mean function (22).

The simulation results in Section VII show that the filtering performance is not sensitive to the parameters of the tail.

VI. THE ROBUST GAUSSIAN FILTER

In the previous section we found the optimal measurement feature for a linear Gaussian measurement model with additive fat tails. The GF can hence be enabled to work with fat-tailed measurement models by filtering in feature space.

Algorithm 1 Gaussian Filter

Input: $p(x_{t-1}|y_{1:t-1}), y_t, g(\cdot), h(\cdot)$ **Output:** $p(x_t|y_{1:t})$

- 1: $p(x_t|y_{1:t-1}) = \text{predict}[p(x_{t-1}|y_{1:t-1}), g(\cdot)]$
 - 2: $p(x_t|y_{1:t}) = \text{update}[p(x_t|y_{1:t-1}), h(\cdot), y_t]$
 - 3: Return $p(x_t|y_{1:t})$
-

Algorithm 2 Robust Gaussian Filter

Input: $p(x_{t-1}|y_{1:t-1}), y_t, g(\cdot), h(\cdot), h^b(\cdot), h^t(\cdot)$ **Output:** $p(x_t|y_{1:t})$

- 1: $p(x_t|y_{1:t-1}) = \text{predict}[p(x_{t-1}|y_{1:t-1}), g(\cdot)]$
 - 2: $\mathcal{N}(y_t|\mu_{y_t}^b, \Sigma_{y_t}^b) = \text{predict}[p(x_t|y_{1:t-1}), h^b(\cdot)]$
 - 3: Given $\mu_{y_t}^b, \Sigma_{y_t}^b$ the feature $\varphi_t(\cdot)$ is defined by (36).
 - 4: $p(x_t|y_{1:t}) = \text{update}[p(x_t|y_{1:t-1}), \varphi_t(h(\cdot)), \varphi_t(y_t)]$
 - 5: Return $p(x_t|y_{1:t})$
-

This robustification can be applied to any member of the family of GFs, be it the EKF or an SPKF. We will refer to the filter obtained by using the feature (36) as the Robust Gaussian Filter (RGF).

For nonlinear, fat-tailed models, the RGF will not be optimal, but it provides a good approximation in the same way the standard GF provides a good approximation to nonlinear, thin-tailed measurement models. If the RGF is applied to a measurement model without a fat tail, it will coincide with the standard GF, since the feature reduces to a linear function (37). Hence, the RGF extends the GF, it broadens its domain of applicability to fat-tailed measurement models.

A. Algorithm

For clarity, we write the RGF algorithm here step by step. Since this involves variables of several time steps, we will reintroduce the time indices which we dropped earlier.

Algorithm 1 shows the steps performed by the standard GF. The input to the algorithm are the previous belief, the new measurement y_t , the state transition model (1) and the measurement model (2). The GF simply predicts, then updates, and finally returns the new estimate.

The RGF Algorithm 2 requires the same inputs as the GF, and additionally the separate models for the body $h^b(\cdot)$ and the tail $h^t(\cdot)$. The RGF delegates all the main computations to the basis GF through the `predict[·]` and the `update[·]` functions. The overhead in the implementation and in the computational cost is minor. Hence, the proposed method makes it simple to robustify any existing GF algorithm.

VII. SIMULATION RESULTS

In this section we evaluate the RGF through simulation. We use Monte Carlo as method for numeric integration. The parameters of the tail assumed by the RGF are kept fixed throughout all simulations.

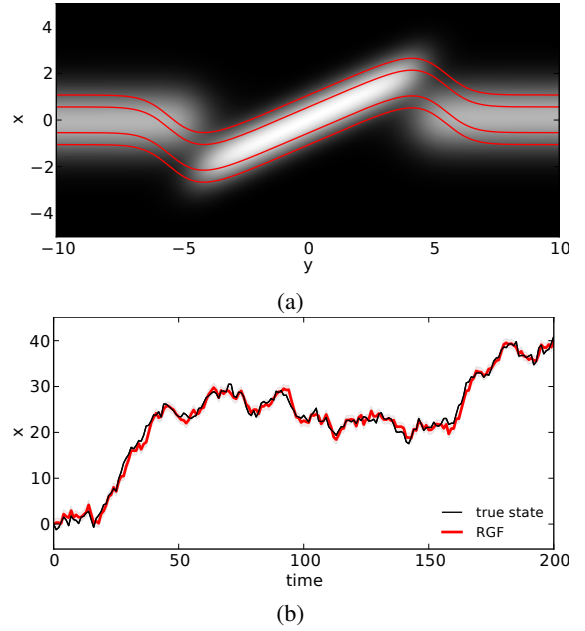


Fig. 5: RGF applied to a fat-tailed measurement process. (a) The contour lines of the approximate density $q(x_1|y_1)$ overlaid on the exact density $p(x_1|y_1)$. (b) True state and filter estimates over time.

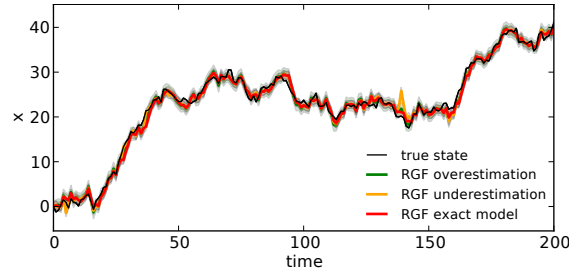


Fig. 6: Robustness of the RGF to the choice of tail parameters. The RGF behaves very similarly even when the tail parameters are severely under- or overestimated.

A. Application to a Linear Filtering Problem

We revisit the simulation in Example 4.1 applying this time the RGF, using the true state transition and measurement model. Comparing Figure 2a to Figure 5a, it is clear that the feature (36) allows for a much better fit of the approximation to the true density. As expected, this improved fit translates to a better filtering performance (Figure 5b). As desired, the proposed method is sensitive to measurements close to the expected values, but does not react to extreme values.

B. Robustness to Tail Parameters

To show that the RGF is not sensitive to the specific choice of the tail parameters, we simulate the same system as above, varying the tail parameters of the model used by the filter. First, we apply a RGF using a measurement model matching the true measurement process, i.e. with tail parameters $\omega = 0.1, \gamma = 10$. Then, we apply two RGFs which use incorrect tail parameters. In one case we make

	value	units		value	units
Δ	0.05	s	$\sigma_{\text{nom},r}$	0.5	km
σ_v	$5 \cdot 10^{-3}$	km/s ²	$\sigma_{\text{con},r}$	15.8	km
β_0	0.59	1/km	$\sigma_{\text{nom},\theta}$	0.63	mrad
H_0	13.4	km	$\sigma_{\text{con},\theta}$	200	mrad
Gm_0	$3.986 \cdot 10^5$	km ³ /s ²	α	0.15	
R_0	6374	km			

TABLE I: Simulation parameters.

both the relative the frequency and scale of the tail much lower than in the true distribution: $\omega = 0.001$, $\gamma = 1.0$ (underestimation). In the other case we make them much higher: $\omega = 0.5$, $\gamma = 100.0$ (overestimation). Figure 6 shows almost no degradation in the performance. The key aspect enabling good filtering performance is that the measurement model has a tail which decays slower than the Gaussian distribution, even when the shape of the true tail is not precisely known.

C. Application to a Nonlinear Filtering Problem

Here we consider the problem of tracking the position of a vehicle that enters atmosphere at high altitude and speed using a radar ground station. The main forces acting on the vehicle are the aerodynamic drag and gravity. The measurements provided by the radar are range and bearing angle to the target vehicle. This type of problem has been used before to compare the capability of filters to deal with strong nonlinearities, e.g. [12, 14].

The noise in radar systems is typically referred to as glint noise in the literature, and is known to be non-Gaussian [8, 28, 14, 4, 7]. It has been modelled in different ways: (i) as a Student t distribution, (ii) as a mixture of two zero-mean Gaussian distributions, one with high probability and low variance and another with low probability and high variance, and (iii) as a mixture of Gaussian and Laplacian distributions, see [4] and references within.

In this section, we simulate the same system as in [12], but replace their Gaussian measurement noise with a mixture of two Gaussians as in [14, 4].

State Transition Process: The state consists of the position of the vehicle $(x^{[1]}, x^{[2]})$, its velocity $(x^{[3]}, x^{[4]})$, and an unknown aerodynamics parameter $x^{[5]}$ which has to be estimated. The state dynamics are

$$x_{t+1}^{[1]} = x_t^{[1]} + \Delta x_t^{[2]} \quad (38)$$

$$x_{t+1}^{[2]} = x_t^{[2]} + \Delta x_t^{[3]} \quad (39)$$

$$x_{t+1}^{[3]} = x_t^{[3]} + \Delta(D_t x_t^{[3]} + G_t x_t^{[1]}) + \sqrt{\Delta} \sigma_v v_t^{[1]} \quad (40)$$

$$x_{t+1}^{[4]} = x_t^{[4]} + \Delta(D_t x_t^{[4]} + G_t x_t^{[2]}) + \sqrt{\Delta} \sigma_v v_t^{[2]} \quad (41)$$

$$x_{t+1}^{[5]} = x_t^{[5]}, \quad (42)$$

where $v^{[1]}$ and $v^{[2]}$ follow a standard normal distribution, and Δ is the discretization time step. The drag and gravity coefficients, $D_t = -\beta_t \exp\left(\frac{R_0 - R_t}{H_0}\right) V_t$ and $G_t = -\frac{Gm_0}{R_t^3}$, depend on the distance of the object to the centre of the Earth $R_t = \sqrt{(x_t^{[1]})^2 + (x_t^{[2]})^2}$, its speed $V_t = \sqrt{(x_t^{[3]})^2 + (x_t^{[4]})^2}$, and its unknown ballistic coefficient $\beta_t = \beta_0 \exp(x_t^{[5]})$. Other

quantities such as the nominal ballistic coefficient β_0 and the mass m_0 and radius R_0 of the Earth are constant, see Table I.

Measurement Model: The radar is located at (x_r, y_r) and measures range r_t and bearing angle θ_t to the target object

$$r_t = \sqrt{(x_t^{[1]} - x_r)^2 + (x_t^{[2]} - y_r)^2} + w_t^{[1]} \quad (43)$$

$$\theta_t = 10^3 \arctan\left(\frac{x_t^{[2]} - y_r}{x_t^{[1]} - x_r}\right) + w_t^{[2]} \quad (44)$$

$$w \sim (1 - \alpha)\mathcal{N}(w|0, \Sigma_{\text{nom}}) + \alpha\mathcal{N}(w|0, \Sigma_{\text{con}}). \quad (45)$$

The nominal noise covariance is represented by $\Sigma_{\text{nom}} = \text{diag}([\sigma_{\text{nom},r}^2, \sigma_{\text{nom},\theta}^2])$, and $\Sigma_{\text{con}} = \text{diag}([\sigma_{\text{con},r}^2, \sigma_{\text{con},\theta}^2])$ is the covariance of the contaminating noise component. We use α and covariances similar to [4], see Table I.

Filter Specification: We compare a RGF with two GFs. The three filters use transition models that coincide with the real process (38)–(42).

In problems of this type, the contaminating noise is often not precisely known. Therefore, we make our RGF assume a measurement model as in Example 4.1

$$p_{\text{RGF}}(w) = 0.9 \mathcal{N}(w|0, \Sigma_{\text{nom}}) + 0.1 \mathcal{C}(w|0, \text{diag}([(10\sigma_{\text{nom},r})^2, (10\sigma_{\text{nom},\theta})^2])), \quad (46)$$

which makes use of some knowledge of the nominal noise Σ_{nom} , while the shape of the tail and the mixing weight take default values. Similarly, the first GF only knows about Σ_{nom}

$$p_{\text{GFthin}}(w) = \mathcal{N}(w|0, \Sigma_{\text{nom}}). \quad (47)$$

Even if the true measurement process (45) was known, the GF is not able to produce accurate estimates in systems with large variance. To show this, we apply a second GF which uses the true covariance of the measurement process (45)

$$p_{\text{GFfat}}(w) = \mathcal{N}(w|0, (1 - \alpha)\Sigma_{\text{nom}} + \alpha\Sigma_{\text{con}}). \quad (48)$$

We simulate the system during 100 s, using the integration time step Δ for the predictions and taking radar measurements at 1 Hz. As in [12], the initial state of the system is $x_0 = [6500.4, 349.14, -1.8093, -6.7967, 0.6932]$, and the initial belief for all filters is centred at $\mu_0 = [6500.4, 349.14, -1.8093, -6.7967, 0]$. Note the mismatch between the true ballistic coefficient and the initial belief, i.e. the nominal β_0 .

Results: Figures 7a and 7b respectively show the error in the estimate of $x^{[1]}$ and the corresponding velocity $x^{[3]}$. We do not include the error in the position and velocity along the other dimension, since they look qualitatively similar. We can see that the GF using the nominal variance (yellow) reacts strongly to outliers. The GF using the true variance (green) of the measurement process does not react as strongly. However, due to the large variance, it tracks the true state poorly. In contrast, the RGF (red) is robust to outliers and at the same time tracks the true state well. This translates to a low 2D location error as shown in Figure 7c.

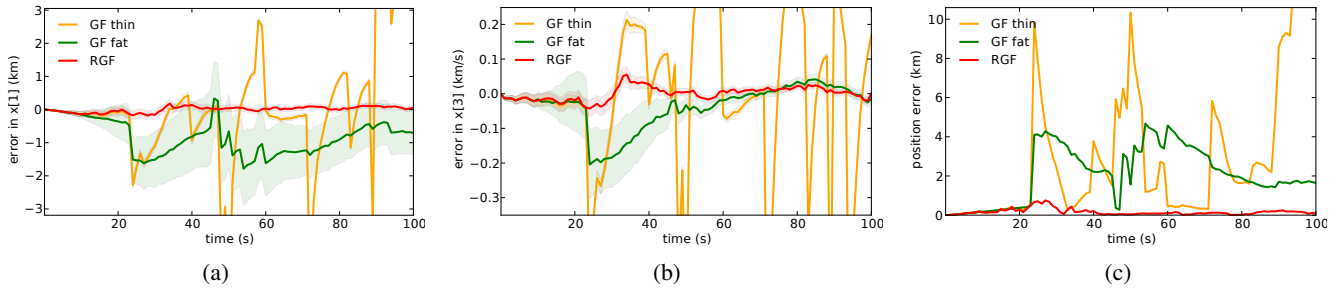


Fig. 7: Results of the nonlinear simulation. The RGF deals well with the nonlinearities and the fat-tailed measurements. (a) Error between the estimated and the true state $x[1]$ (position component), plus/minus one standard deviation of the estimate. (b) Error between estimated and true state $x[3]$ (velocity). (c) Euclidean distance between estimated and true 2D position.

VIII. CONCLUSION

In the standard GF algorithm, the mean estimate is a linear function of the measurement. We showed that for fat-tailed measurement models this provides a very poor approximation to the exact posterior mean.

A recent result [30] showed that filtering in the space of a feature of the measurement can allow for more accurate approximations of the exact posterior. Here, we have found the feature that is optimal for fat-tailed measurement models under certain conditions.

We have shown both theoretically and in simulation that applying the standard GF in this feature space enables it to work well with fat-tailed measurement models. The proposed RGF is hence robust to outliers while maintaining the efficiency of the standard GF. Any member of the family of GFs, be it the EKF or a SPKF, can thus be robustified by the proposed method without changing any of the main computations.

REFERENCES

- [1] G. Agamennoni, J. I. Nieto, and E. M. Nebot. Approximate inference in state-space models with heavy-tailed noise. *IEEE Transactions on Signal Processing*, 2012.
- [2] I. Arasaratnam and S. Haykin. Cubature Kalman filters. *Automatic Control, IEEE Transactions on*, 2009.
- [3] D. Barber. *Bayesian Reasoning and Machine Learning*. Cambridge University Press, 2012.
- [4] I. Bilik and J. Tabrikian. Target tracking in glint noise environment using nonlinear non-Gaussian Kalman filter. In *IEEE Conference on Radar*, 2006.
- [5] R. Cooke, D. Nieboer, and J. Misiewicz. Fat-tailed distributions: Data, diagnostics, and dependence. Technical report, 2011.
- [6] B. de Finetti. La prévision : ses lois logiques, ses sources subjectives. *Annales de l'institut Henri Poincaré*, 1937.
- [7] H. Du, W. Wang, and L. Bai. Observation noise modeling based particle filter: An efficient algorithm for target tracking in glint noise environment. *Neurocomputing*.
- [8] G. A. Hewer, R. D. Martin, and J. Zeh. Robust preprocessing for Kalman filtering of glint noise. *IEEE Transactions on Aerospace and Electronic Systems*, 1987.
- [9] P. J. Huber. Robust estimation of a location parameter. *Annals of Mathematical Statistics*, 1964.
- [10] K. Ito and K. Xiong. Gaussian filters for nonlinear filtering problems. *IEEE Transactions on Automatic Control*, 2000.
- [11] S. J. Julier and J. K. Uhlmann. A new extension of the Kalman filter to nonlinear systems. In *Proceedings of AeroSense: The 11th Int. Symp. on Aerospace/Defense Sensing, Simulations and Controls*, 1997.
- [12] S. J. Julier and J. K. Uhlmann. Unscented filtering and nonlinear estimation. *Proceedings of the IEEE*, 2004.
- [13] R.E. Kalman. A new approach to linear filtering and prediction problems. *Journal of Basic Engineering*, 1960.
- [14] C. D. Karlgaard and H. Schaub. Comparison of several nonlinear filters for a benchmark tracking problem. In *AIAA Guidance, Navigation, and Control Conference and Exhibit*, 2006.
- [15] H. J. Kushner. Approximations to optimal nonlinear filters. *IEEE Transactions on Automatic Control*, 1967.
- [16] C. Masreliez and R. Martin. Robust Bayesian estimation for the linear model and robustifying the Kalman filter. *IEEE Transactions on Automatic Control*, 1977.
- [17] R. J. Meinhold and N. D. Singpurwalla. Robustification of Kalman filter models. *Journal of the American Statistical Association*, 1989.
- [18] M. Nørgaard, N. K. Poulsen, and O. Ravn. New developments in state estimation for nonlinear systems. *Automatica*, 2000.
- [19] R. Piche, S. Särkkä, and J. Hartikainen. Recursive outlier-robust filtering and smoothing for nonlinear systems using the multivariate student-t distribution. In *IEEE International Workshop on Machine Learning for Signal Processing (MLSP)*, 2012.
- [20] M. Roth, E. Ozkan, and F. Gustafsson. A Student's t filter for heavy tailed process and measurement noise. In *IEEE International Conference on Acoustics, Speech and Signal Processing (ICASSP)*, 2013.
- [21] S. Särkkä. *Bayesian filtering and smoothing*. Cambridge University Press, 2013.
- [22] S. Särkkä and A. Nummenmaa. Recursive noise adaptive Kalman filtering by variational Bayesian approximations. *IEEE Transactions on Automatic Control*, 2009.
- [23] I. C. Schick and S. K. Mitter. Robust recursive estimation in the presence of heavy-tailed observation noise. *The Annals of Statistics*, 1994.
- [24] H. W. Sorenson. *Kalman Filtering: Theory and Application*. IEEE Press selected reprint series. IEEE Press, 1960.
- [25] S. Thrun, D. Fox, W. Burgard, and F. Dellaert. Robust Monte Carlo localization for mobile robots. *Artificial Intelligence*, 2001.
- [26] J.-A. Ting, E. Theodorou, and S. Schaal. A Kalman filter for robust outlier detection. In *IEEE/RSJ International Conference on Intelligent Robots and Systems (IROS)*, 2007.
- [27] R. van der Merwe and E. Wan. Sigma-Point Kalman Filters for probabilistic inference in dynamic state-space models. In *In Proceedings of the Workshop on Advances in Machine Learning*, 2003.
- [28] W.-R. Wu and P.-P. Cheng. A nonlinear IMM algorithm for maneuvering target tracking. *IEEE Transactions on Aerospace and Electronic Systems*, 1994.
- [29] Y. Wu, D. Hu, M. Wu, and X. Hu. A numerical-integration perspective on Gaussian filters. *IEEE Transactions on Signal Processing*, 2006.
- [30] M. Wüthrich, S. Trimpe, D. Kappler, and S. Schaal. A New Perspective and Extension of the Gaussian Filter. In *Robotics: Science and Systems (R:SS)*, 2015.